

Longitudinal $\bar{\Lambda}_0$ polarization in heavy-ion collisions as a probe for QGP formation

G. Herrera^{1,a}, J. Magnin^{2,b}, L.M. Montaño^{1,c}

¹ Depto. de Física del Centro de Investigación y de Estudios Avanzados del IPN, Apartado postal 14-740, México D.F. 07000, México

² Centro Brasileiro de Pesquisas Físicas, Rua Dr. Xavier Sigaud 150 – CEP 22290-180, Rio de Janeiro, Brazil

Received: 21 September 2004 / Revised version: 25 October 2004 /
 Published online: 17 December 2004 – © Springer-Verlag / Società Italiana di Fisica 2004

Abstract. We present an analysis of the longitudinal $\bar{\Lambda}_0$ polarization in ultrarelativistic heavy-ion collisions. The polarization of $\bar{\Lambda}_0$'s coming from the decay chain $\bar{\Xi} \rightarrow \bar{\Lambda}_0 + \pi$ exhibits a very well differentiated behavior depending on the production region of the primordial $\bar{\Xi}$'s. This effect reflects the different values of the $N_{\bar{\Xi}}/N_{\bar{\Lambda}_0}$ ratio in the QGP region, where nucleon–nucleon interactions take place in a hot and dense environment, and the peripheral region, in which ordinary nucleon–nucleon interactions occur. An increase in the longitudinal $\bar{\Lambda}_0$ polarization signals a strangeness enhancement which is thought of as a property of the QGP phase.

1 Introduction

In nuclear collisions at relativistic and ultrarelativistic energies, a phase transition from ordinary nuclear matter to a quark gluon plasma (QGP) is expected, which should be observed when sufficiently high baryonic densities and/or temperatures are achieved in the collision. In order to identify this phase transition, a number of experimental observables, namely J/ψ suppression, strangeness enhancement, fluctuations in particle ratios, flow patterns, etc. have been proposed [1].

In particular, it has been argued that the strangeness enhancement in hot and dense regions of nuclear matter would lead to an abundant formation of multistrange baryons and antibaryons, providing thus key information about the QGP formation [2]. Indeed, detailed calculations [3] predict that the abundance of $\bar{\Xi}(\bar{s}s\bar{q})$ should be enriched to about half the abundance of antihyperons $\bar{Y}(\bar{s}\bar{q}\bar{q})$ as compared to the $\bar{\Xi}/\bar{Y}$ ratio seen in nucleon–nucleon interactions. Considering that at $\sqrt{s} = 63$ GeV, $\bar{\Xi}/\bar{\Lambda}_0 = 0.06 \pm 0.02$ [5] in the central rapidity region, then in the presence of QGP, the $\bar{\Xi}/\bar{\Lambda}_0$ would be 10 times greater. However, although the $\bar{\Xi}/\bar{\Lambda}_0$ ratio is a quantity which is difficult to establish experimentally, the longitudinal $\bar{\Lambda}_0$ polarization is not and can be used to get a measurement of the above mentioned ratio [2].

At this point it is useful to remember that $\bar{\Xi}$ decays into $\bar{\Lambda}_0 + \pi$ with a branching fraction of about 99% and that the weak decay polarizes the $\bar{\Lambda}_0$ spin longitudinally.

This means that all the longitudinally polarized $\bar{\Lambda}_0$ are associated with the primordial abundance of $\bar{\Xi}$. Note also that the $\bar{\Omega}^+$ have little influence on the particle abundances and, in particular, on their polarizations [2]. In fact, the STAR Collaboration [4] measured $N_{\Omega^-}/N_{\bar{\Xi}^+} \sim 0.16$, where N_{Ω^-} refers to the total number of $\Omega^- + \bar{\Omega}^+$. Furthermore, the polarization of $\bar{\Lambda}_0$'s coming from $\bar{\Omega}^+ \rightarrow \bar{\Lambda}_0 + K^+$ (BR $\sim 68\%$) is a factor of 5 lower than the polarization of $\bar{\Lambda}_0$'s coming from $\bar{\Xi} \rightarrow \bar{\Lambda}_0 + \pi$ while the polarization of the $\bar{\Lambda}_0$'s coming from the decay $\bar{\Omega}^+ \rightarrow \bar{\Xi} + \pi$ (BR $\sim 23\%$ and BR $\sim 9\%$ for the $\bar{\Xi}^0$ and the $\bar{\Xi}^+$ decay modes respectively) and the subsequent decay of the $\bar{\Xi}$ into $\bar{\Lambda}_0 + \pi$ is still lower by a factor of ~ 20 . This situation is expected to be maintained at the energy where QGP formation takes place (see also the discussions in [2, 3]).

The $\bar{\Lambda}_0$ polarization can be defined in terms of the so called up–down asymmetry of the $\bar{\Lambda}_0$ decay with reference to the plane normal to the $\bar{\Lambda}_0$ momentum. Thus [2]

$$\frac{N_u - N_d}{N_u + N_d} = \frac{1}{2} \alpha_{\bar{\Lambda}} p_{\bar{\Lambda}}, \quad (1)$$

where $p_{\bar{\Lambda}} = \alpha_{\bar{\Xi}} = -\alpha_{\Xi}$ is the $\bar{\Lambda}_0$ polarization and $\alpha_{\bar{\Lambda}}$ is the $\bar{\Lambda}$ decay parameter. From data tables $\alpha_{\bar{\Lambda}} = -\alpha_{\Lambda} = 0.642 \pm 0.013$ and $\alpha_{\bar{\Xi}} = 0.413 \pm 0.022$ (0.455 ± 0.015) for $\bar{\Xi}^0$ ($\bar{\Xi}^-$). Hence the total up–down asymmetry for all the neutral $\bar{\Lambda}_0$ events is

$$\frac{N_u - N_d}{N_u + N_d} = \gamma \frac{1}{2} \alpha_{\bar{\Lambda}} \alpha_{\bar{\Xi}}, \quad (2)$$

where $\gamma = N_{\bar{\Xi}}/N_{\bar{\Lambda}_0}$.

Equation (2) shows that in ordinary nucleon–nucleon interactions at the ISR energies, the up–down asymmetry

^a e-mail: gherrera@fis.cinvestav.mx

^b e-mail: jmagnin@cbpf.br

^c e-mail: lmontano@fis.cinvestav.mx

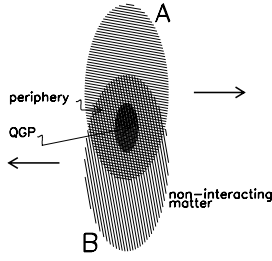


Fig. 1. Schematic representation of the reaction $A + B$ and the regions in which Ξ 's are produced. In the hot and dense (QGP) region, $\gamma_{\text{QGP}} \sim 0.5$ while in the periphery, in which ordinary nucleon–nucleon interactions take place, $\gamma_{\text{periph.}} \ll \gamma_{\text{QGP}}$

should be of the order of -0.008 while in hot and dense nuclear matter it should amount to something of about -0.07 , which is an effect of one order of magnitude and one that could be measured in experiments.

Of course, all of the above argumentation can be applied to Λ_0 and the Ξ 's, but in this case, many of the Λ_0 's should be mere fragments of nucleons going into $\Lambda_0 K$, giving a less clear signal.

In the interaction region of a heavy-ion collision it is expected that one has a core of hot and dense nuclear matter – possibly QGP – surrounded by a region in which ordinary nucleon–nucleon interactions take place (see Fig. 1). These regions, as it is shown in the following sections, can be mapped by measuring the $\bar{\Lambda}_0$ polarization as a function of the impact parameter, b , and transverse momentum, p_T . What is expected is a plot displaying a polarization approximately constant and of the order of -0.07 in the hot and dense region surrounded by a region in which the polarization is again constant, and of the order of -0.008 , corresponding to the periphery, where ordinary nucleon–nucleon interactions occur.

This paper is organized as follows. In Sect. 2 we study the behavior of the $N_{\Xi}/N_{\bar{\Lambda}_0}$ ratio in both the low and high nuclear density regions. In Sect. 3 we calculate the $\bar{\Lambda}_0$ polarization as a function of the impact parameter and transverse momentum, and Sect. 4 is devoted to conclusions and final remarks.

2 The $N_{\Xi}/N_{\bar{\Lambda}}$ ratio in heavy-ion collisions

In the interaction region of the collision of nucleus A and B , when QGP coexists with the ordinary nuclear matter, the ratio of the number of Ξ to the number of $\bar{\Lambda}_0$ baryons is given by

$$\begin{aligned} \gamma_{A+B} &= \frac{N_{\Xi}^{\text{periph.}} + N_{\Xi}^{\text{QGP}}}{N_{\bar{\Lambda}_0}^{\text{periph.}} + N_{\bar{\Lambda}_0}^{\text{QGP}}} \\ &= \frac{N_{\bar{\Lambda}_0}^{\text{periph.}} \gamma_{\text{periph.}} + N_{\bar{\Lambda}_0}^{\text{QGP}} \gamma_{\text{QGP}}}{N_{\bar{\Lambda}_0}^{\text{periph.}} + N_{\bar{\Lambda}_0}^{\text{QGP}}}, \end{aligned} \quad (3)$$

where the quantities labeled periph. and QGP refer respectively to the number of $\bar{\Lambda}_0$ and Ξ in each region. As long as the dependence on the impact parameter, b , and transverse momentum, p_T , of $N_{\bar{\Lambda}_0}$ is different in the QGP from the peripheral region, γ_{A+B} must be also dependent on b and p_T . In fact, in the same way as the longitudinal polarization

of the $\bar{\Lambda}_0$'s does, it should provide a map of the interacting region in which the peripheral and QGP zones are displayed. Note, however, that the only dependence on b and p_T in γ_{A+B} arises from the dependence on b and p_T in $N_{\bar{\Lambda}_0}^{\text{periph.}}$ and $N_{\bar{\Lambda}_0}^{\text{QGP}}$ since $\gamma_{\text{periph.}}$ and γ_{QGP} are expected to be approximately constant [5].

2.1 $N_{\bar{\Lambda}_0}(b, p_T)$ in the peripheral region

The $N_{\bar{\Lambda}_0}^{\text{periph.}}$ can be estimated along the lines in [6]. As stated in [6], and remembering that in ordinary nucleon–nucleon interactions the typical behavior of the production cross section as a function of p_T is an exponential in p_T^2 , the number of produced $\bar{\Lambda}_0$'s as a function of the impact parameter and p_T in the collision of nucleus A and B can be written as

$$\frac{d^4 N_{\bar{\Lambda}_0}^{\text{periph.}}}{d^2 b dp_T^2} = \frac{1}{2} C e^{-ap_T^2} T_{AB}(b), \quad (4)$$

where the $1/2$ is because the number of $\bar{\Lambda}_0$'s is approximately half the number of neutral hyperons, C is a constant which normalizes the integral over the transverse momentum to unity, and T_{AB} is

$$T_{AB}(z, \mathbf{b}) = \int d^2 s T_A(z, \mathbf{b}) T_B(z, \mathbf{s} - \mathbf{b}), \quad (5)$$

with T_A and T_B given by

$$T_A(z, \mathbf{s}) = \int_{-z/2}^{z/2} dz' \rho_A(z', \mathbf{s}), \quad (6)$$

and where the limits of integration over z have to be extended to $[-\infty, +\infty]$. For ρ_A , which is the nucleon density per unit area in the transverse plane with respect to the collision axis, we use the standard Woods–Saxon density profile

$$\rho_A(\mathbf{r}) = \frac{\rho_0}{1 + e^{(r-R_A)/d}}, \quad (7)$$

with $R_A = 1.1A^{1/3}$ fm, $d = 0.53$ fm [7] and ρ_0 fixed by normalization:

$$\int d\mathbf{r} \rho_A(\mathbf{r}) = A, \quad (8)$$

giving $\rho_0 = 0.17 \text{ fm}^{-3}$ in the case of ^{197}Au , which we shall consider as an example in the following.

We are assuming that each peripheral collision produces final state particles in the same way as in free nucleon reactions. However, in order to exclude the zone where the density of participants n_p is above the critical density n_c to produce QGP, we rewrite (4) as

$$\begin{aligned} \frac{d^4 N_{\bar{\Lambda}_0}^{\text{periph.}}}{d^2 b dp_T^2} &= \\ &= \frac{1}{2} C e^{-ap_T^2} \int d^2 s T_A(z, \mathbf{b}) T_B(z, \mathbf{s} - \mathbf{b}) \Theta[n_c - n_p(\mathbf{s}, \mathbf{b})], \end{aligned} \quad (9)$$

where $n_p(\mathbf{s}, \mathbf{b})$ is the density of participants at the point \mathbf{s} and Θ is the step function. The density of participants per unit transverse area in the collision of nucleus A with nucleus B at an impact parameter \mathbf{b} has a profile given by [8]

$$n_p(s, \mathbf{b}) = \quad (10)$$

$$T_A(\mathbf{s}) \left[1 - e^{-\sigma_{NN} T_B(s-\mathbf{b})} \right] + T_B(\mathbf{s}-\mathbf{b}) \left[1 - e^{-\sigma_{NN} T_A(\mathbf{s})} \right],$$

where σ_{NN} is the nucleon–nucleon inelastic cross section which we take as $\sigma_{NN} = 32$ mb. The total number of participants N_p at impact parameter b is

$$N_p(b) = \int d^2s n_p(\mathbf{s}, \mathbf{b}). \quad (11)$$

From (9), the number of $\bar{\Lambda}_0$'s coming from the decay chain $\bar{\Xi} \rightarrow \bar{\Lambda}_0 + \pi$ is then given by

$$\frac{d^4 N_{\bar{\Xi} \rightarrow \bar{\Lambda}_0 + \pi}^{\text{periph.}}}{d^2b dp_T^2} = \gamma_{\text{periph.}} \frac{d^4 N_{\bar{\Lambda}_0}^{\text{periph.}}}{d^2b dp_T^2}. \quad (12)$$

Following [8], we choose $n_c = 3.3 \text{ fm}^{-2}$ for the critical density. This number results from the observation of a substantial reduction of the J/Ψ yield in Pb–Pb collisions at the SPS. For the parameter a in (4) and (9) there are no published data at the relevant energies, which for LHC should be about 5 TeV per nucleon. Then we use the value measured by the Hera-B Collaboration [9] in proton–nucleus interactions at 920 GeV, $a = 2.2 \pm 0.3 \text{ GeV}^{-2}$.

2.2 $N_{\bar{\Lambda}}(b, p_T)$ in the QGP region

In QGP, the average number of produced antistrange quarks scales with the number of participants N_p^{QGP} in the collision roughly as [11]

$$\frac{\langle \bar{s} \rangle}{N_p^{\text{QGP}}} = c N_p^{\text{QGP}}. \quad (13)$$

Assuming that a \bar{s} quark will produce $\bar{\Xi}$, $\bar{\Lambda}_0$ or $\bar{\Sigma}_0$, and taken the number of $\bar{\Lambda}_0$ approximately equal to the number of produced $\bar{\Sigma}_0$, we have

$$\langle \bar{s} \rangle = 2N_{\bar{\Xi}}^{\text{QGP}} + 2N_{\bar{\Lambda}_0}^{\text{QGP}} = [2\gamma_{\text{QGP}} + 2] N_{\bar{\Lambda}_0}^{\text{QGP}}. \quad (14)$$

Combining (13) and (14) we obtain

$$N_{\bar{\Lambda}_0}^{\text{QGP}} = \frac{c}{2\gamma_{\text{QGP}} + 2} [N_p^{\text{QGP}}]^2. \quad (15)$$

N_p^{QGP} as a function of the impact parameter is given, using (11), as

$$N_p^{\text{QGP}}(b) = \int d^2s n_p(\mathbf{s}, \mathbf{b}) \theta[n_p(\mathbf{s}, \mathbf{b}) - n_c]. \quad (16)$$

Equation (15) represents the behavior of the number of $\bar{\Lambda}_0$ as a function of the impact parameter; then we use

$$\frac{d^4 N_{\bar{\Lambda}_0}^{\text{QGP}}}{d^2b dp_T^2} = \frac{c}{2\gamma_{\text{QGP}} + 2} [N_p^{\text{QGP}}(b)]^2 C' e^{-a' p_T^2}, \quad (17)$$

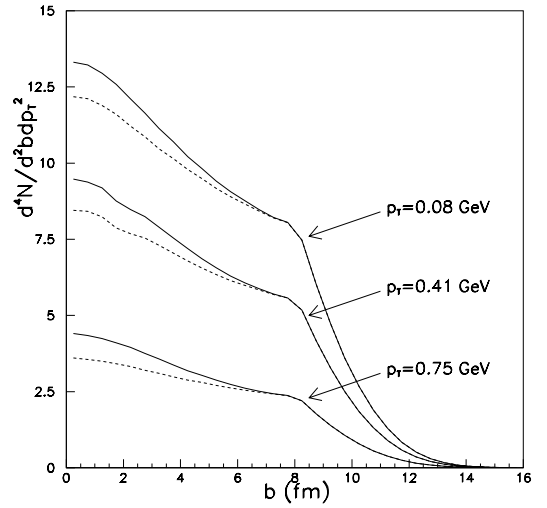


Fig. 2. Number of $\bar{\Lambda}_0$'s as a function of the impact parameter for fixed values of p_T . A full line shows the total (peripheral + QGP) number. A dashed line is the peripheral contribution

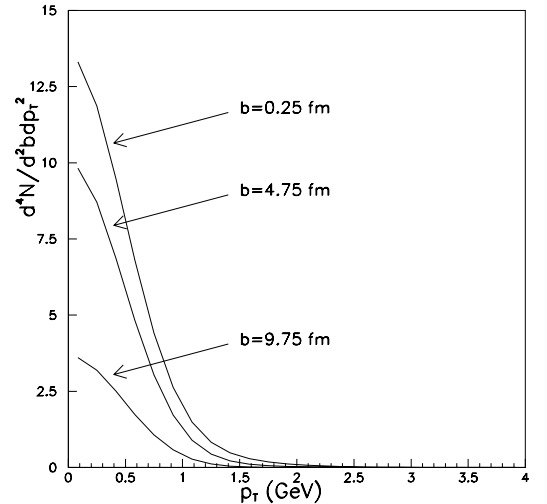


Fig. 3. Number of $\bar{\Lambda}_0$'s as a function of p_T at fixed values of b

assuming an exponential dependence in p_T^2 for $\bar{\Lambda}_0$ production [10]. As for the peripheral $\bar{\Lambda}_0$'s, (17) times γ_{QGP} gives the number of $\bar{\Lambda}_0$'s as a function of b and p_T coming from the decay chain $\bar{\Xi} \rightarrow \bar{\Lambda}_0 + \pi$ in the QGP phase. We use $c = 0.005$ [6] and read $a' = 0.67$ from [10].

In Figs. 2 and 3 we show the behavior of the total (peripheral + QGP) number of $\bar{\Lambda}_0$'s as a function of the impact parameter for different values of p_T and as a function of p_T for several values of b respectively.

3 $\bar{\Lambda}$ polarization in heavy-ion interactions

The up–down asymmetry is then given by (2) with γ_{eff} as given in (3) and shown in the left side of Fig. 4 as a function of b and p_T . The right side of Fig. 4 shows the behavior of $\gamma_{\text{eff}} = N(\bar{\Xi})/N(\bar{\Lambda}_0)$ defined in (3) as a function of b and p_T . As can be seen, the $\bar{\Lambda}_0$ polarization exhibits a dramatical change as the impact parameter becomes bigger

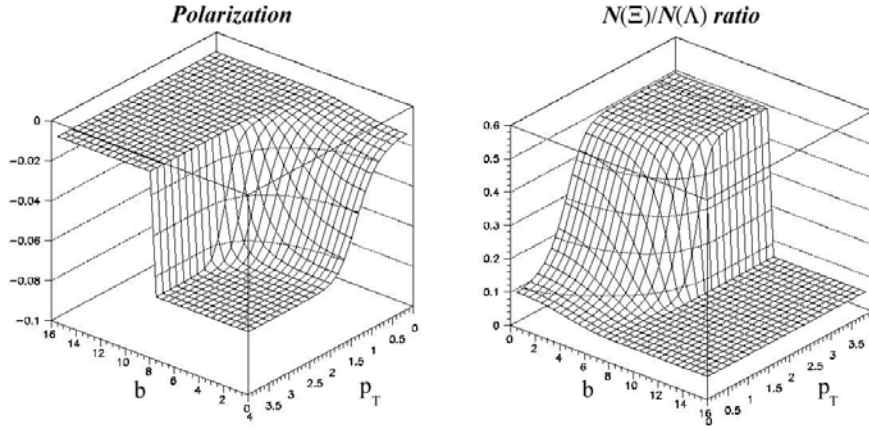


Fig. 4. Left: $\bar{\Lambda}_0$ polarization as a function of b and p_T as defined in (2). We used $\gamma^{\text{periph.}} = 0.06$ and $\gamma^{\text{QGP}} = 0.5$ to obtain the plot. Right: $\gamma_{\text{eff}} = N(\bar{\Xi})/N(\bar{\Lambda}_0)$ as a function of b and p_T as defined in (3). Note that this plot is rotated by 180° with respect to the plot of the polarization for a better visualization. The maximum of γ_{eff} corresponds to the minimum of the $\bar{\Lambda}_0$ polarization

than a critical value, starting from which the QGP region suddenly vanishes. From this value on the polarization reaches the characteristic value seen in ordinary nucleon–nucleon interactions. Conversely, at high p_T and low b , the polarization shows the behavior expected in the hot and high density region where QGP takes place. This reflects the characteristic increase in the $N_{\bar{\Xi}}/N_{\bar{\Lambda}_0}$ expected when QGP be formed. Another interesting feature of the longitudinal $\bar{\Lambda}_0$ polarization is the dependence on p_T due to the different p_T dependence of $\bar{\Lambda}_0$ production in the peripheral and QGP region.

However, in relativistic heavy-ion collisions, there are several effects which can modify the $\bar{\Lambda}_0$ polarization and have to be taken properly into account. These are

- (i) $\bar{\Lambda}_0$'s produced by secondary pion–nucleon scattering,
- (ii) secondary scattering of $\bar{\Lambda}_0$'s with nucleons in the interaction region and
- (iii) spin-flip in secondary interactions of the $\bar{\Lambda}_0$'s. $\bar{\Lambda}_0$'s coming from secondary pion–nucleon interactions will have a characteristic low momentum signature and can be eliminated from the analysis by setting kinematical constrains in the reconstruction of the data, therefore excluding them from the polarization analysis. Spin-flip effects in polarization, which are associated to spin–spin interactions among the $\bar{\Lambda}_0$ and the surrounding particles, are characterized by a polarization transfer coefficient which expresses the final polarization in terms of the initial one as

$$P' = DP. \quad (18)$$

However, due to the lack of experimental information at the range of energies of interest, we will omit this effect from our analysis (for a more detailed analysis and references, see [6]). Secondary scattering of the $\bar{\Lambda}_0$'s with nucleons in the surrounding nuclear environment will produce a momentum shift that can be characterized in terms of a sequential model. The final effect will be that a $\bar{\Lambda}_0$ produced with an initial (p_L, p_T) , after multiple scattering, in the high energy limit, will have an average momentum [6]

$$\begin{aligned} \langle p_L(b) \rangle &= p_L e^{-I\bar{N}(b)}, \\ \langle p_T(b) \rangle &= p_T e^{-I\bar{N}(b)} \cos \left[\Gamma \sqrt{\bar{N}(b)} \right], \end{aligned} \quad (19)$$

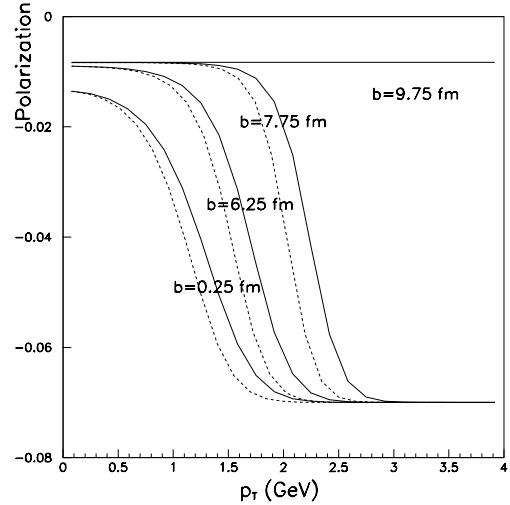


Fig. 5. $\bar{\Lambda}_0$ polarization as a function of p_T at several values of the impact parameter. A full line shows the polarization before the momentum shift due to multiple scattering in the nuclear medium, a dashed line shows the polarization after the momentum shift

where $I = 0.2$ is the inelasticity coefficient, $\Gamma = 0.01$ is the average dispersion angle in each collision and $\bar{N}(b)$ is the average number of $\bar{\Lambda}_0$ collisions in the nuclear medium,

$$\bar{N}(b) = \sigma_{\bar{\Lambda}_0 N}^{\text{tot}} T_A(b/2), \quad (20)$$

where $\sigma_{\bar{\Lambda}_0 N}^{\text{tot}} = 1.4 \text{ mb}$ [9], taken from proton–nucleon interactions at 920 GeV. This effect is shown in Fig. 5 where the polarization as a function of p_T is displayed for several values of b before and after the momentum shift due to multiple scattering. Note also that, for low p_T , the polarization takes the value corresponding to that expected in ordinary nucleon–nucleon interactions, a behavior which is more evident as b grows. Conversely, at high p_T and low b , the polarization reaches the value expected in the QGP phase.

4 Final remarks and conclusions

In conclusion, we have shown that the longitudinal polarization of $\bar{\Lambda}_0$ in heavy-ion relativistic interactions presents

a dramatical change with $N_{\bar{\Xi}}/N_{\bar{\Lambda}_0}$ in the transition from the expected QGP region to the peripheral one. This effect, which can be easily measured in the laboratory, can help to unveil one of the signals of the transition to the QGP phase, namely the strangeness enhancement and the consequent increase in the multistrange baryon formation. Notice that the longitudinal polarization of the $\bar{\Lambda}_0$ in the low b , high p_T region gives direct access to the measurement of the γ_{QGP} ratio. It is simply the quotient of the polarization by $\alpha_{\bar{\Lambda}}\alpha_{\bar{\Xi}}/2$. Conversely, in the high b , high p_T region, the $\bar{\Lambda}_0$ longitudinal polarization gives the γ_{periph} ratio, which is not easily measured in experiments. It is interesting to note that the momentum shift due to multiple scattering of $\bar{\Lambda}_0$'s in the nuclear medium produces a small increase in the polarization as a function of p_T in the low momentum region.

Another possible observable which would exhibit strong changes in the presence of the QGP phase is the transverse polarization of the Λ_0 's [6, 12]. However, in this case a decrease is expected of its value with respect to what happens in p - p interactions since the transverse polarization is related to the production mechanisms of the Λ_0 .

Acknowledgements. This work was supported by a binational research agreement CNPq/CONACYT under grant numbers 690176/02-3 and J200-652. J.M. is grateful for the warm hospitality at the Physics Department of CINVESTAV, where part of this work was done. L.M.M. is grateful for the kind hospitality at CBPF during the completion of this work

References

1. For a recent review on the subject, see U.W. Heinz, Hunting down the Quark Gluon Plasma in relativistic heavy-ion collisions, Proceedings of the Conference on Strong and Electroweak Matter (SEWM 98), Copenhagen, Denmark, edited by J. Ambjorn, P. Damgaard, K. Kainulainen, R. Rummukainen (World Scientific Publ. Co., Singapore 1999), p. 81
2. M. Jacob, J. Rafelski, Phys. Lett. B **190**, 173 (1987); M. Jacob, Z. Phys. C **38**, 273 (1988)
3. P. Koch, B. Müller, J. Rafelski, Phys. Rep. **142**, 167 (1986)
4. J. Adams et al. (STAR Collaboration), Phys. Rev. Lett. **92**, 182301 (2004)
5. T. Åkesson et al. (ISR-Axial-Field Spectrometer Collaboration), Nucl. Phys. B **246**, 1 (1984)
6. A. Ayala, E. Cuautle, G. Herrera, L.M. Montaño, Phys. Rev. C **65**, 024902 (2002); Rev. Mex. Fis. **48**, 549 (2002)
7. B. Povh, C. Scholz, K. Rith, F. Zersche, Particles and nuclei: an introduction to the physical concepts, p. 65 (Springer, Berlin 1995)
8. J.P. Blaizot, J.Y. Ollitrault, Phys. Rev. Lett. **77**, 1703 (1996)
9. I. Abt et al. (Hera-B Collaboration), Eur. Phys. J. C **29**, 181 (2003)
10. C. Adler et al. (STAR Collaboration), Phys. Rev. Lett. **89**, 092301-1 (2002)
11. J. Letessier, J. Rafelski, A. Tounsi, Phys. Lett. B **389**, 586 (1996)
12. A.D. Panagiotou, Phys. Rev. C **6**, 1999 (1986)